Supplementary Information (SI) for ChemComm.

Monitoring UV radiation Dosage based on Deuterated Luminescent Hydrogen-organic frameworks

Mengjia Yuan,[a], Fuyin Ma,*[a] Zhen Jiang,[a] Lixi Chen,[a] Zhifang Chai,[a] and Shuao Wang*[a]

[†]State Key Laboratory of Radiation Medicine and Protection, School for Radiological and Interdisciplinary Sciences (RAD-X) and Collaborative Innovation Center of Radiation Medicine of Jiangsu Higher Education Institutions, Soochow University, Suzhou 215123, China.

S1. Experimental section.

Materiels.

Tris(4-bromophenyl)amine (LR, purified by sublimation), Potassium Carbonate (AR, 99%), Dicyandiamide (AR, 98%) were purchased from TCI Development Co., Ltd. 4-Cyanophenylboronic acid (BR, 99%), Tetrakis(triphenylphosphine)-palladium (metals basis, 99%) and Potassium hydroxide (BR, 85% KOH basis) were obtained from Sigma-Aldrich Co., Ltd. Sodium sulfate anhydrous, potassium carbonate. 2-Methoxyethanol Dimethyl Sulfoxide-D_6, 99.5 atom% D and Deuterium oxide 95 atom% D were purchased from J&K Scientific Co., Ltd. 2-Methoxyethanol (GC, 99%) was purchased from Aladdin Co., Ltd. Dichloromethane (AR), Ethyl acetate (AR), N,N-Dimethylformamide (AR) and Methanol (AR) were purchased from Chinasun Specialty Products Co., Ltd. Aceton (AR) was purchased from Yonghua Chemical Co., Ltd. through the materials supply center of Soochow University.

All reagents and solvents were used in this work without further purification.

Analytical methods.

Powder X-ray diffraction (PXRD). The PXRD data were collected from 5 to 50° with a step of 0.02° and the time for data collection was 0.2 s on a Bruker D8 Advance diffractometer with Cu Kα radiation (λ=1.54056 Å)

Single Crystal X-ray diffraction (SC-XRD). Single crystal data collection was performed on a Bruker D8-Venture diffractometer with a Turbo X-ray Source (Cu–Kα radiation, λ = 0.71073 Å), adopting the direct-drive rotating anode technique and a CMOS detector at room temperature. The data frames were collected using the program APEX4 and processed using the program SAINT routine in APEX4.

Fourier translation infrared (FT-IR). The FT-IR spectra of the samples were recorded in the range of 4000-400 cm^{-1} by a Thermo Nicolet IS 50 spectrometer.

Photoluminescence spectra (PL). The single crystal solid-state photoluminescence and UV-vis absorption spectra were recorded on a Craic Technologies microspectrophotometer; Crystals were placed on a quartz slide, and data was collected after auto-set optimization. When the 365 nm excitation light was selected, an optical filter masking signal below 420 nm was applied in order to mask the interference of excitation light.

Thermofravimetric analysis (TGA). Thermalgravimetric analysis was carried out on a NETZSCH STA 449 F3 jupiter instrument in the range of 25 - 900°C under a nitrogen flow at a heating rate of 10 °C/ min.

Scanning electron microscopy (SEM). All SEM images of the as-prepared HOFs materials were acquired with the voltage of 10 kV using a field-emission scan electron microscope (FE-SEM, thermo scientific Apreo 2C) under vacuum and all samples were coated with gold to improve the electronic conductivity.

CO_2 adsorption-desorption measurements. For porosity analysis, the CO_2 adsorption-desorption experiments of the as-prepared HOFs were conducted on a Micromeritics ASAP 2460 Surface Area and Porosimetry Analyzer at 273 K by using ultra-high purity CO_2. The original samples were exchanged by fresh methanol three times a day and degassed at 120°C for 12 h before the measurements.

1H nuclear magnetic resonance (NMR). 1H NMR spectra were all recorded at 600 MHz on either an Agilent Technologies DD2-600 spectrometer.

Elementar Analysensysteme (EA). All analysis was collected on Elementar Unicube by CHNS patterns.

Theoretical Calculation. The absorption and emission spectra of the hydrogen-bonded organic framework (HOF) were simulated using Gaussian 16 software, which employed density functional theory (DFT) for the optimization of molecular structures. The B3LYP functional was utilized for structural optimization, with the 6-31G(d) basis set and D3 dispersion correction to ensure stability. Both the ground state and the first excited state (S1) structures were optimized using the same functional and basis set. Molecular orbital analyses were carried out using Multiwfn, while molecular mapping was performed with Visual Molecular Dynamics (VMD). Additionally, charge transfer behavior was extensively analyzed through Multiwfn.

S2. Experimental section.

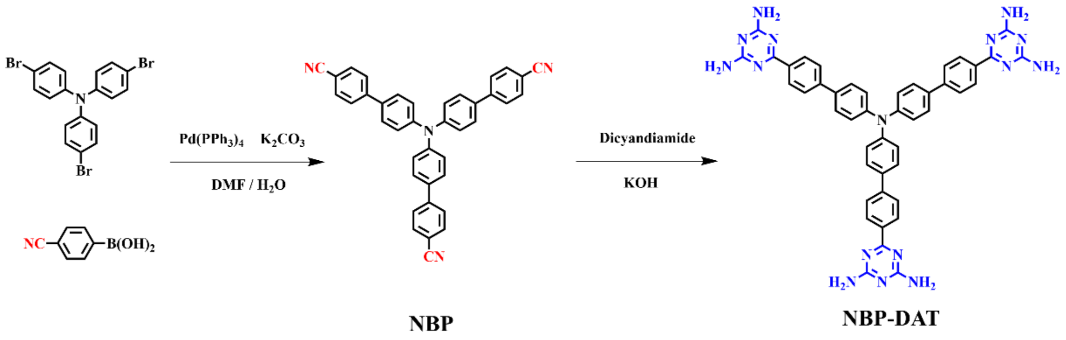

Scheme 1. The synthesis of NBP-DAT.

Synthesis of 4',4''',4'''''-nitrilotris(([1,1'-biphenyl]-4-carbonitrile)) (NBP). 4-Cyanophenyboronic acid (1.043 g, 7.095 mmol) and tris(4-bromophenyl)amine (0.816 g, 1.693 mmol) were added into a 50 mL flask under the nitrogen atmosphere. Then DMF (30 mL), anhydrous potassium carbonate aqueous solution (K_2CO_3, 1.32 g, 9.551 mmol) and deionized water (48 mL) were added. At last, Pd(PPh_3)$_4$ (0.156 g, 0.135 mmol) was added into the above reaction system. The mixture was kept at 90ºC under nitrogen atmosphere for 48 h. After the reaction was finished, the mixture was cooled to room temperature and then dissolved in CH_2Cl_2. The organic phase was extracted with water three times, after that organic phase was dried by anhydrous Na_2SO_4. The volatiles were then removed by vacuum evaporation. Compound NBP (80.0% yield) was obtained as a yellow solid via the purified by silica gel column (CH_2Cl_2/petroleum ether = 2:1). The spectroscopic data match well with those reported previously.

Synthesis of 6-(4'-(bis(4'-(4,6-diamino-1,3,5-triazin-2-yl)-[1,1'-biphenyl]-4-yl)amino)-[1,1'-biphenyl]-4-yl)-1,3,5-triazine-2,4-diamine (NBP-DAT). 4',4''',4'''''-nitrilotris(([1,1'-biphenyl]-4-carbonitrile)) (0.175 g, 0.319 mmol), dicyandiamide (0.18 g, 2.143 mmol) and 2-Methoxyethanol (15 mL) were mixed into a flask at room temperature. After stirring for 30 min in the N_2 atmosphere, KOH (0.03 g, 0.536 mmol) was added into the reaction mixture, which then was heated under reflux for 24 h. After the reaction, the mixture was cooled to room temperature, and then filtered to collect the product. The compound NBP-DAT (84% yield) obtained yellow powder was washed with deionized water and methyl for three times. The hydrogen spectrum data and spectroscopic data match with those reported previously.

Procedure for the preparation of HHOF and DHOF.

Synthesis of HHOF.

The NBP-DAT (10 mg) was dissolved in 10 mL of heated DMF (at 90 ºC). Deionized water (3 mL) was added and then the mixture was placed at 70 ºC for 7 d. The bright yellow crystals of HHOF grew on the bottom.

Synthesis of DHOF.

The NBP-DAT (10 mg) was dissolved in 10 mL of heated DMF (at 90 ºC). Deuterium oxide (3 mL) was added and then the mixture was placed at 70 ºC for 7 d. The bright yellow crystals of DHOF grew at the bottom.

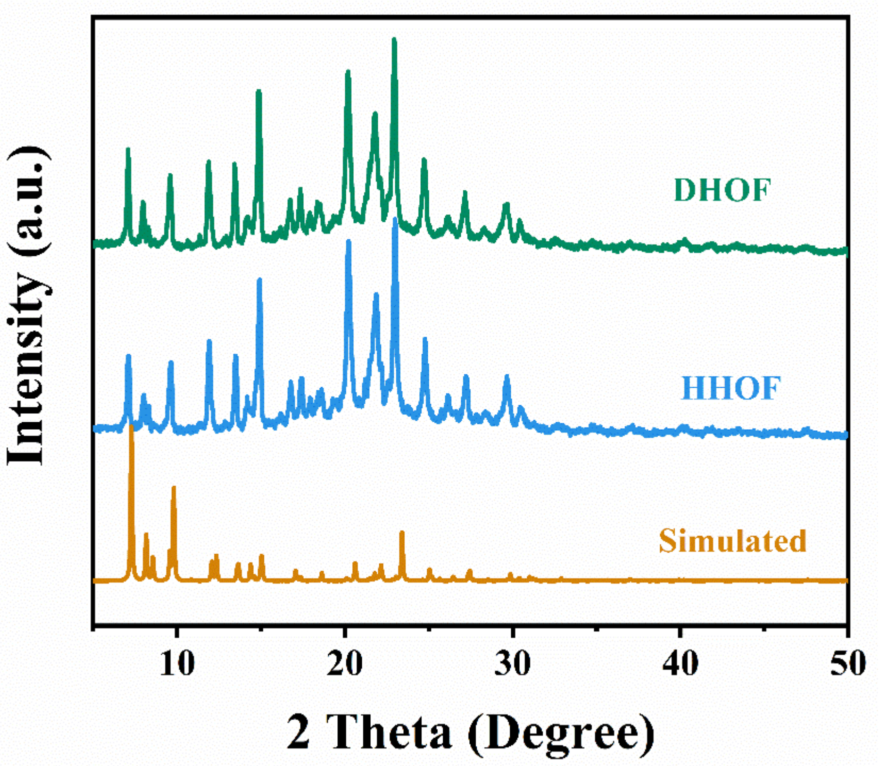

Figure S1. The PXRD spectra of HHOF (light blue line) and DHOF (green line).

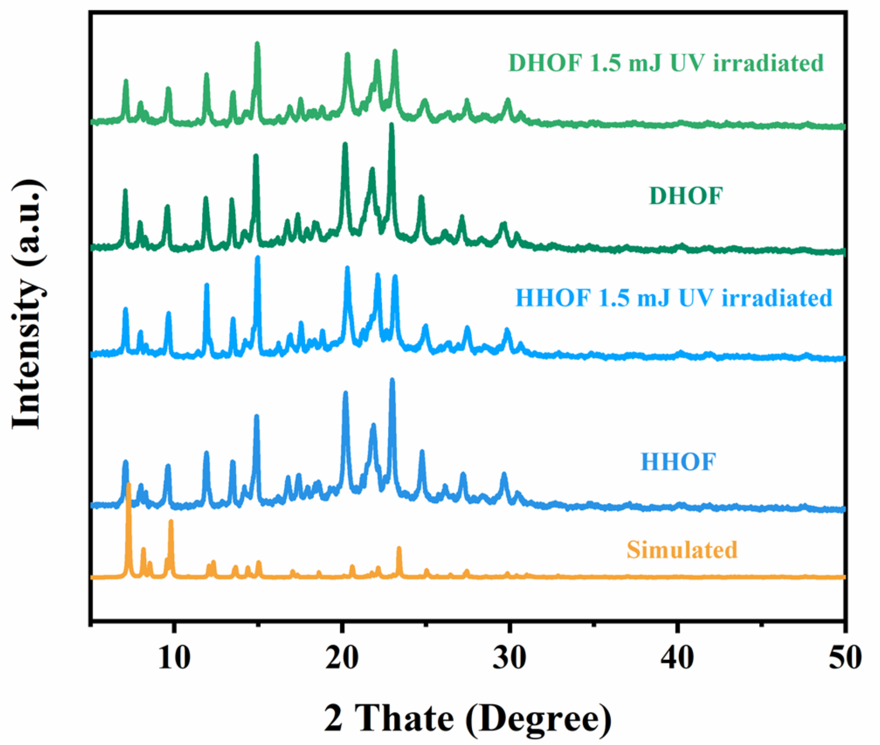

Figure S2. PXRD patterns of DHOF and HHOF after treatment with 1.5 mJ UV irradiation, respectively.

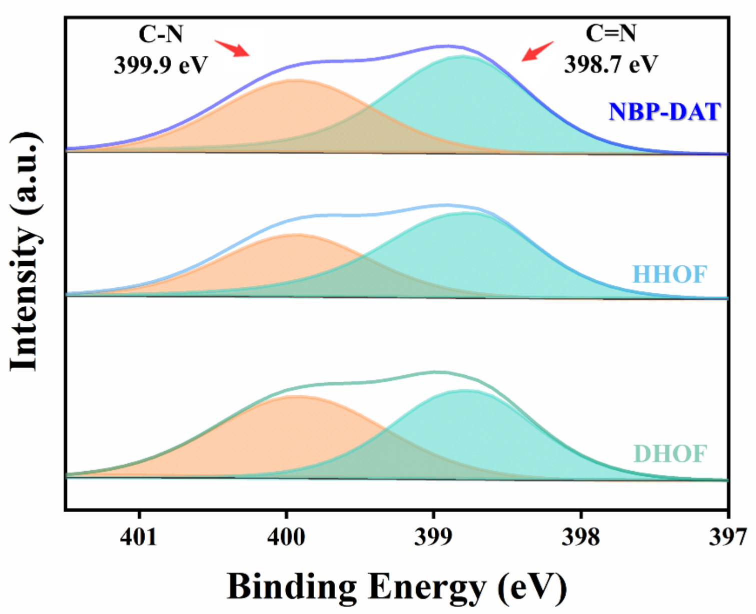

Figure S3. XPS patterns of NBP-DAT, HHOF and DHOF.

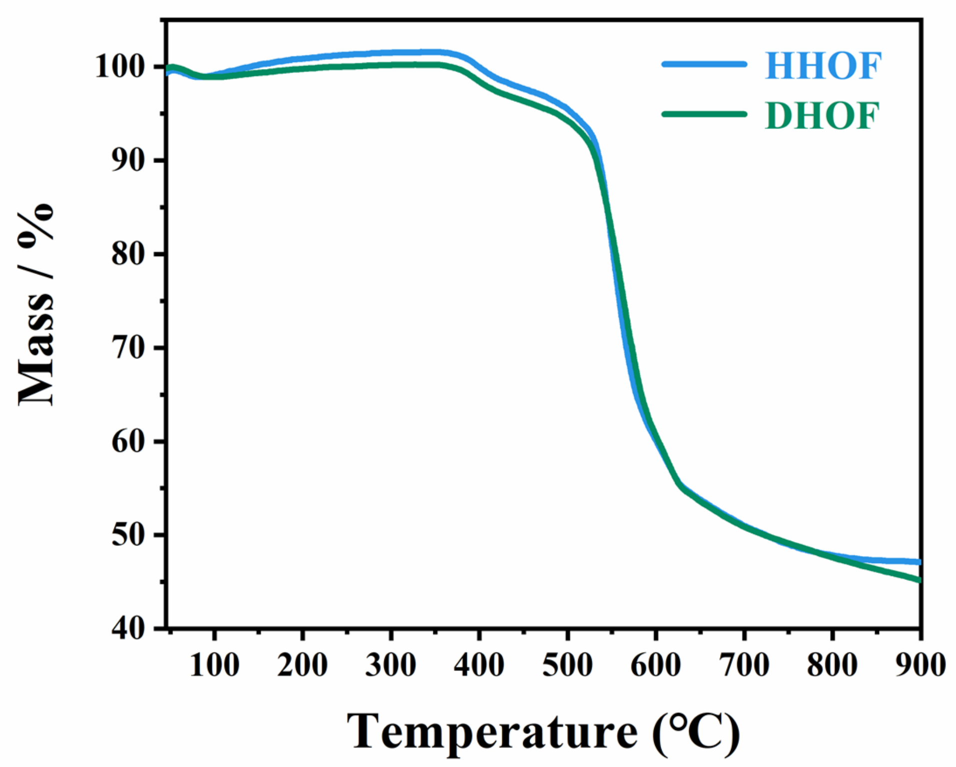

Figure S4. The thermogravimetric analysis curves of DHOF (green line) and HHOF (blue line).

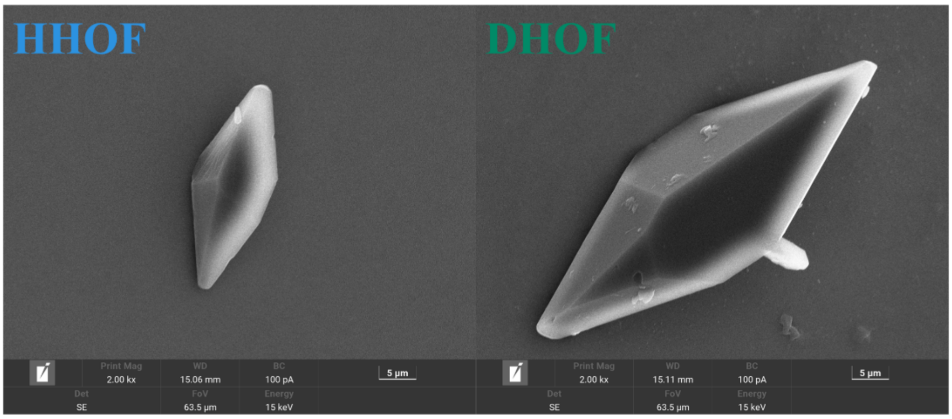

Figure S5. SEM images of HHOF and DHOF.

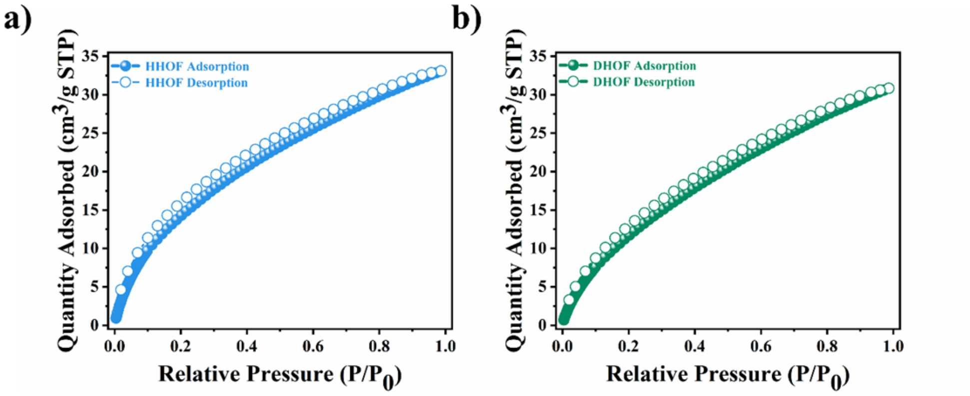

Figure S6. The CO_2 adsorption/desorption isotherms a) HHOF and b) DHOF at 273 K.

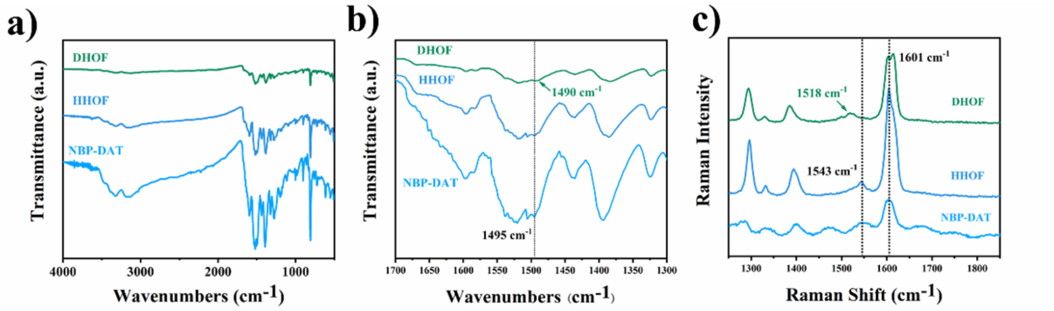

Figure S7. a) FT-IR spectra of NBP-DAT (pale blue), HHOF (blue) and DHOF (green). b) FT-IR spectra of N-H. c) Raman Shift of NBP-DAT (pale blue), HHOF (blue) and DHOF (green), 1601 cm^{-1}: benzene.

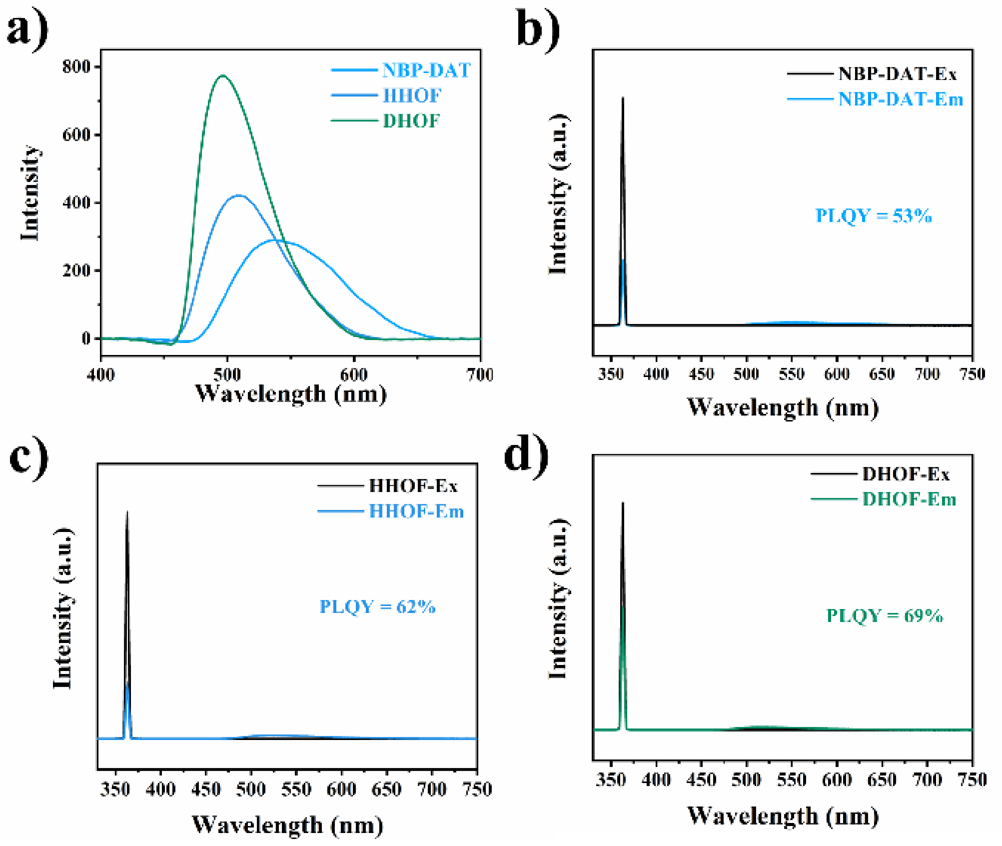

Figure S8. a) The PL spectra of NBP-DAT, HHOF and DHOF. b) c) d) The PLQY of NBP-DAT, HHOF and DHOF.

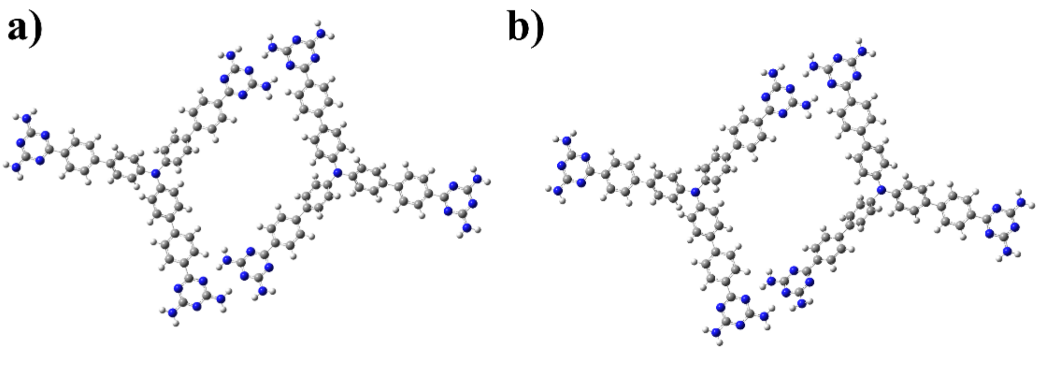

Ground state

Excited state

Figure S9. The most stable structure of the hydrogen-bonding dimer in the ground and excited states.

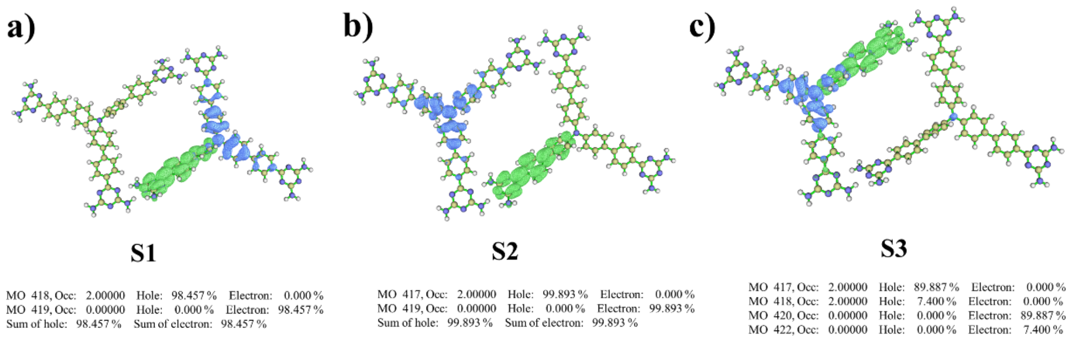

Figure S10. Hole-electron orbital isosurfaces of hydrogen-bonded dimer in S1, S2 and S3 excited states. (Blue and green isosurfaces represent hole and electron distributions, respectively.)

Table S1. Isotopic mass spectrometry

	^{2}H atom%
HHOF	0.0216
DHOF	0.0504

Table S2. Elemental analysis

	C%	N%	H%
HOF-Calcd.	67.5	28.0	4.5
HHOF	62.6	25.3	4.9
DHOF	60.1	24.4	4.8

Table S3. The relationship between emission intensity (y) and UV dose (x) of HOFs.

	Equation	R-Square(R^2)	LOD ($\times 10^{-7}$ J)
HHOF	$y=4363.63x+0.06$	0.99	2.44
DHOF	$y=5915.18x+0.18$	0.98	1.02

Table S4. The detail data of UV detection limit for reported porous crystalline frameworks.

Sample	LOD (× 10^{-7} J)	Reference
$UO_2(L)(DMF)$	2.4	1
$[Hphen]_2[(UO_2)_2(ox)_3]$	0.069	2
CP-1-Tb	24	3
CP-2-Tb	3.2	3
CP-3-Tb	180	3
$[(TEA)_2(UO_2)_5(PhPC)_6$	39	4
Tb-DBTPA	0.091	5
HHOF	2.44	This work
DHOF	1.02	This work

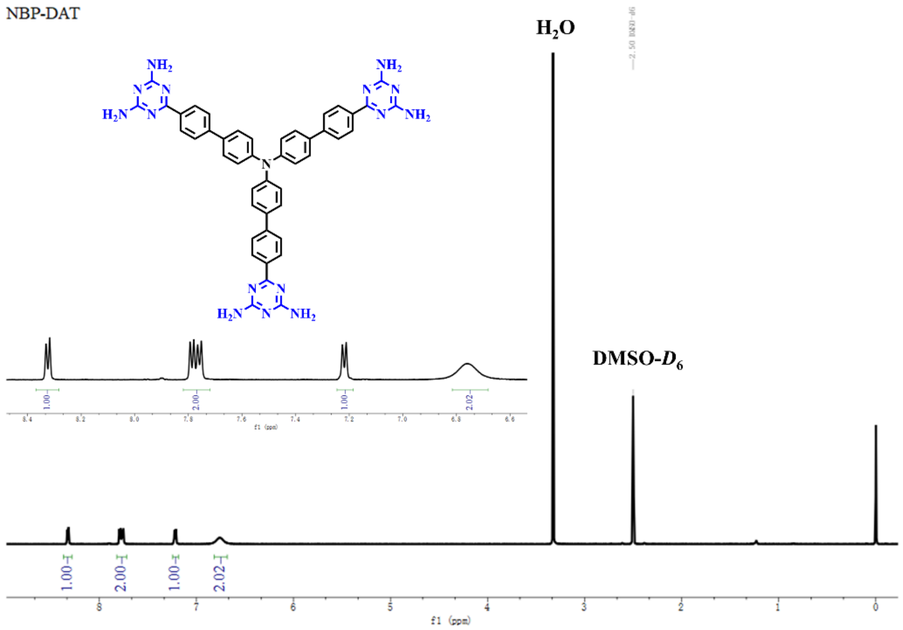

Figure S11. ^1H NMR of NBP-DAT (DMSO-D_6, DD2-600 MHz).

The impact of crystal number, solvent presence in the channels, and crystal size on photoluminescence intensity was examined. To eliminate the potential influence of residual solvents in the material's channels, the as-synthesized HOFs (HHOF and DHOF) were subjected to solvent exchange with ethanol. As shown in Figure S12, after performing UV irradiation tests on a large number of crystals, the data indicate that DHOF still exhibits a superior UV fluorescence detection limit (DHOF = 1.77 $\times 10^{-7}$ J, HHOF = 2.73 $\times 10^{-7}$ J).

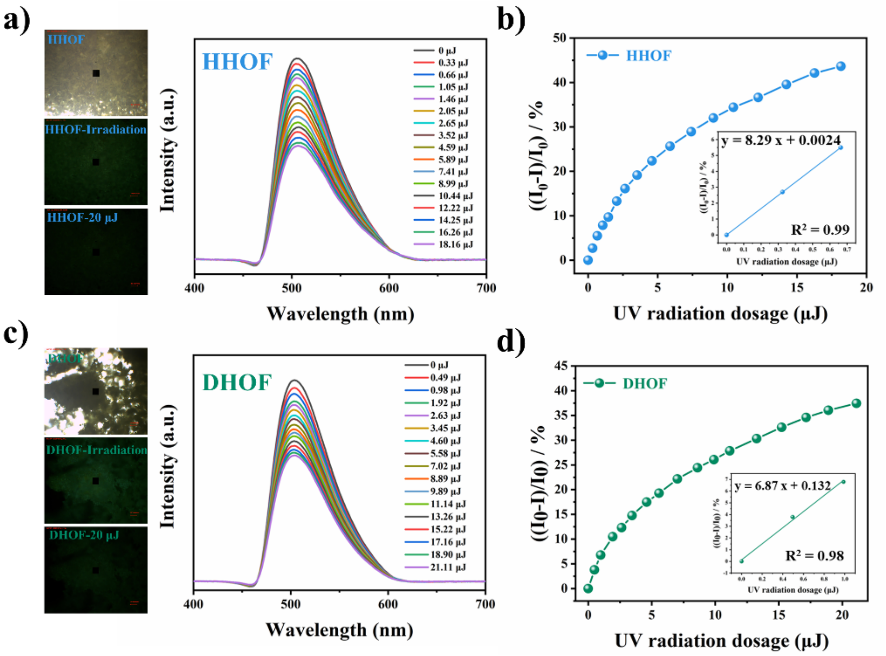

Figure S12. a) Left: The photoluminescence figures of HHOF (top: Non-irradiated, down: Irradiated), Right: UV dosage-dependent photoluminescence spectra of HHOF. b) Plot showing the relative photoluminescence enhancing process (measured at 512 nm) of HHOF (Insite: Data points in the low dose range are fitted in a linear relationship). c) Left: The photoluminescence figures of DHOF (top: Non-irradiated, down: Irradiated), Right: UV dosage-dependent photoluminescence spectra of DHOF. d) Plot showing the relative photoluminescence enhancing process (measured at 512 nm) of DHOF (Insite: Data points in the low dose range are fitted in a linear relationship).

Reference

(1) W. Liu, X. Dai, J. Xie, M. A. Silver, D. Zhang, Y. L. Wang, Y. W. Cai, J. Diwu, J. Wang, R. H. Zhou, Z. F. Chai, and S. A. Wang, *ACS Appl. Mater. Interfaces*, **2018,** 10, 4844-4850.

(2) J. Xie, Y. A. Wang, D. Zhang, C. Y. Liang, W. Liu, Y. Chong, X. M. Yin, Y. G. Zhang, D. X. Gui, L. H. Chen, W. Tong, Z. Y. Liu, J. Diwu, Z. F. Chai, and S. A. Wang, *Chem. Commun.*, **2019,** 55, 11715-11718.

(3) Z. F. Zheng, H. J. Lu, Y. M. Wang, H. L. Bao, Z. J. Li, G. P. Xiao, J. Lin, Y. Qian, and J. Q. Wang, *Inorg. Chem.*, **2021,** 60, 1359-1366.

(4) L. Chen, L. H. Chen, Y. G. Zhang, J. Xie, J. Diwu, *J Inorg. Mater.*, **2020,** 35, 1391-1397.

(5) S. D. Zhang, L. X. Chen, J, Xie, Y. G. Zhang, F. H. Xia, X. Wang, K. Li, F. W. Zhai, Q. Yang, L. H. Chen, Y. X. Wang, X. Dai, Z. F. Chai, and S. A. Wang, *Inorg. Chem.*, **2022,** 61, 4561-4565.